ORIGINAL RESEARCH

Effect of the humidity on analysis of aromatic compounds with planar differential ion mobility spectrometry

Andriy Kuklya · Florian Uteschil · Klaus Kerpen · Robert Marks · Ursula Telgheder

Abstract In this paper, we demonstrate that humidity is a crucial parameter for analysis of aromatic compounds of low polarity with planar differential ion mobility spectrometry. Utilization of polar modifiers which are usually applied for the improvement of separation ability of DMS based systems does not improve the separation of aromatic compounds. Moreover, the peak area of the model compounds decreases with the increase of the modifier (water vapors and 2-propanole) concentration. The influence of the polar modifiers on the DMS separation ability was proven on examples of the six aromatic compounds (BTEX, 1,2,4-trimethylbenzene (TMB), and naphthalene) and one aliphatic compound (hexane). The influence of the modifier concentration on the compensation voltage, peak area, and peak width was investigated and discussed. The strong influence of the proton affinity of analytes on the peak area in the measurements with modifiers was demonstrated. Some notable aspects of the formation of the reactant ion positive are demonstrated and discussed.

A. Kuklya (✉) · F. Uteschil · K. Kerpen · R. Marks · U. Telgheder
Department of Instrumental Analytical Chemistry, University of Duisburg-Essen (UDE), Universitätsstraße 5, 45141 Essen, Germany
e-mail: andriy.kuklya@uni-due.de

U. Telgheder
IWW Water Centre, Moritzstr. 26, 45476 Mülheim a.d. Ruhr, Germany

Introduction

The importance of the development of new analytical methods for the analysis of aromatic compounds cannot be overstated. Continuously increasing production and use of fossil fuels have significantly increased the contamination of water resources, particularly groundwater and aquifers. The contamination of aquifers and groundwater by fuels constitute an environmental issue of major concern worldwide and may lead to risk of drinking water supply [1, 2]. Due to the leaking of oil tanks and pipelines the groundwater is contaminated by petroleum products such as gasoline, diesel fuel and heating oil. This is the one of the most common sources for contamination of groundwater with BTEX (benzene, toluene, ethylbenzene, xylenes) and PAHs (polycyclic aromatic hydrocarbons). BTEX accounts for as much as 90 % of the gasoline components that are found in the water-soluble fraction, when a gasoline contacts with the water [3]. The total contribution of all C3-benzene isomers was found to be about 1 % of the total aromatics. The same study demonstrates that naphthalene and its methylated derivatives are the dominating compounds in the water fraction among the others PAHs which were found in trace amounts. Therefore, BTEX, 1,2,4-trimethylbenzene (TMB), and naphthalene were chosen as a model compounds for this study.

Most of the existing methods for the analysis of gasoline contaminated samples include the GC or LC pre-separation steps [4]. Despite the fact that the chromatography is an effective and well-established method, in the case of the complex samples it can be very time consuming. The methods based on the ion mobility can significantly enhance the chromatographic separation or even be considered as an alternative to the chromatography [5, 6].

The differential ion mobility spectrometry (DMS), also known as planar high field asymmetric waveform

ion mobility spectrometry (FAIMS), is a rapidly advancing technology that is both sensitive and fast, operates at atmospheric pressure, and provides a unique type of selectivity, which is orthogonal to most of other separation techniques [7, 8]. In contrast to the conventional Time of Flight Ion Mobility Spectrometry (ToF-IMS), in which the separation of ions is based on specific coefficients of ion mobility in a uniform electric field, DMS separates ions based on a nonlinear dependence of the mobility coefficient on the electric field strength.

The dependence of the ion mobility coefficient on the electric field can be explained by the reversible cluster formation model, which describes field dependent cluster formations that lead to variation of the average ion cluster cross section [9]. The functional principles of the DMS are described elsewhere [10, 11].

Initially, in the most of DMS/FAIMS applications the gaseous samples were analysed. Over the last years, however, a number of applications for DMS/FAIMS-MS coupling [8, 12], as well as stand-alone DMS/FAIMS for direct liquid sample analysis [13, 14], were presented. In case of the direct measurements of the liquid samples the increased level of the humidity in the DMS can be expected. In case of the polar compounds of high proton affinity the increased humidity does not lead to the reduction in the sensitivity and can even results in increased separation power of the DMS [14].

Recently it was demonstrated that addition of the appropriate amount of volatile organic compounds (modifiers) to the transport gas can significantly enhance the resolving power of planar DMS [12, 15–17]. For curved geometries the introduction of a solvent vapor of high concentration is problematic, since the focusing effect causes a dramatic decrease in ion signal or even a complete signal loss. [18, 19]. The intensity of the ion signal in the spectrometers with planar electrodes geometry is not as affected by solvent vapors due to the lack of ion focusing effect. Typically polar modifiers (e.g. 2-propanol, acetone, ethylacetate, acetonitrile, water vapors etc.) were utilized for improvement of the spectrometer resolving power. It is assumed that polar modifiers may induce the cluster/decluster mechanism, which provides increasing of the ion separation in comparison with the measurements with pure nitrogen. The separation efficiency is dependent on the strength of the interaction between the analyte and the modifier.

In this paper, we demonstrate that utilization of polar modifiers (e.g. 2-propanol and water vapor) which are usually applied for the improvement of separation ability of DMS based systems does not improve the separation of aromatic compounds. Moreover, the peak area of the model compounds decreases with the increase of the modifier concentration.

Experimental

Experimental setup

The principle scheme of the experimental setup used in this study is shown in Fig. 1. The overall nitrogen flow entering the DMS was prepared by mixing the main flow of pure nitrogen, controlled by a mass flow controller (MFC, Pneutronics, VSO-GC), with an additional nitrogen flow containing the modifier (water vapors or 2-propanol). The main flow of the pure nitrogen was dried over molecular sieves (4 Å, Typ 514, Roth). The homemade vapor generator (VG) included a temperature controlled saturated vapor source and a flow of nitrogen. The nitrogen flow containing the moisture was controlled by a mass flow controller (GFC17, 0–50 mL min^{-1} N$_2$, Aalborg, USA). The overall nitrogen flow, controlled by a solid state flow meter (Restek 6000, Restek, UK) located on the exhaust of DMS, was kept constant at 270 mL min^{-1}. The pressure was monitored using the pressure sensor from the DMS, which is built on the input to the analyzer. The humidity was measured with MDM-300 advanced dew-point hydrometer (Michell Instruments, UK). The minimum humidity level reached with the current setup was 6.5 ppm$_v$.

Chemicals

To check the influence of the modifier concentration on the compensation voltage and signal area seven compounds of low polarity were selected. Six of these compounds, namely benzene (AppliChem, 99+ %), toluene (J.T. Baker, 99.9 %), ethylbenzene (Fluka, 99+ %), p-xylene (Fluka, 99+ %), 1,2,4-trimethylbenzene (Aldrich, 98 %), and naphthalene (Sigma-Aldrich, 99 %) represent aromatic compounds. n-Hexane (Sigma, 97+ %) was taken to compare the behavior of the aromatic and aliphatic compounds in the presence of modifiers. Water was prepared by treating of deionized water with purelab ultra (Elga). To compare the behavior of the compounds of low and high polarity in the presence of humidity, 2-hexanone (Sigma-Aldrich, 98 %) was taken as a representative compound of high polarity. The molecular weights, the
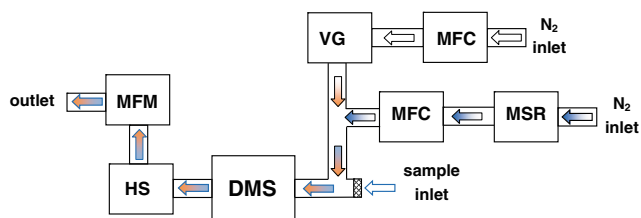

Fig. 1 The principle scheme of the experimental setup: differential ion mobility spectrometer (DMS), humidity sensor (HS), mass flow controller (MFC), mass flow meter (MFM), molecular sieves reservoir (MSR), vapor generator (VG)

proton affinities, and the vapor pressures of the model compounds are summarized in Table 1.

The samples for the measurements were prepared as follows: an analyte sample volume of 1 ml was transferred into a 20 mL vial under nitrogen atmosphere. The vial was closed with the screw cap equipped with Butyl/PTFE septa (S/N 100032, BGB, Germany) and equilibrated for a 1 h at 20 °C. Each sample was a mixture of 0.5 μL of the headspace over the analyte and 4.5 μL of the nitrogen (99.999 %, Air Liquide, Germany). 0.5 μL of the sample was introduced using 5 μL syringe (SGE, Australia) by manual injection through a silicone/PTFE septum (VWR, Germany).

DMS

The differential ion mobility spectrometer (SVAC-V, ^{63}Ni 185 MBq, Scionex Corp., USA) settings were as follows: sensor temperature =80 °C, number of steps =100, step duration =10 ms, step settle time =3 ms, steps to blank =1. The measurements were analysed in the positive (positive ions) mode at RF-Voltage of 1000 V (20 kV cm^{-1}) and nitrogen (99.999 %, Air Liquide, Germany) flow rate of 270 mL min^{-1}, otherwise noted. For the compounds demonstrating a significant shift on the CV scale (2-hexanone) the compensating voltage range was set from −43 to +5 V. For other compounds the range from −10 to +5 V was set in order to achieve a better resolution.

For each sample, five single measurements were recorded using Sionex Expert software (version 2.4.0). For the determination of peak parameters (centre, area, FWHM) the measured data were analysed by the fityk (version 0.9.4) program [20]. The peaks were fitted with Gaussian functions using the Levenberg-Marquardt algorithm.

It should be noted that the analyte signal positions on the compensation voltage scale are very sensitive to even minor pressure differences. To enable the comparison of spectra obtained under different experimental conditions the method described by Nazarov et al. [21] was used. This method proposes utilization of E/N scaling in Townsend units (Td). In our study, utilization of this method has minimized but not completely eliminated the differences between the measurements at different pressures. That is why the data presented in this manuscript were recorded at the narrow pressure gap between 14.40 and 14.54 psi.

Results and discussion

### Effects of the humidity on the reactive ion positive (RIP)

The relationship between the RIP compensation voltage (CV), the RIP area, the RIP FWHM, and the humidity are demonstrated in Fig. 2. The shift of the RIP toward more negative CV with the increase of the humidity was observed within the humidity range of 20 to 550 ppm$_v$. This shift is in a good agreement with the reversible cluster formation model. However, for humidities lower than 20 ppm$_v$ the opposite relationship between CV and humidity was observed (see Fig. 2, top). Additionally, a substantial increase of the RIP area was observed within the same humidity range.

The observed effects can be explained by the following model. In the nitrogen of very low humidity (few ppm$_v$ and less) the water has a minor influence on the positive ion charge carriers. In this humidity range, the positive ion charge carriers are represented by ions of a relatively low lifetime ($[N_2(H_2O)_n]^+$, $[NO(H_2O)_n]^+$, $n=0,1$; etc. [22]) and only a minor part of the positive charges are represented by H_3O^+. This results in a very weak RIP signal. With increase of water vapor concentration the amount of the water clusters increases, increasing with it the role of relatively long leaving water clusters as the charge carriers. This leads to the observed increase of the RIP area (see Fig. 2, top and Fig. 3). In this range of humidity (up to 20 ppm$_v$), however, the water

Table 1 List of compounds used in the current study with the corresponding molecular weights, proton affinities, and vapor pressures

Compound	MW [g mol^{-1}]	Proton Affinity [kJ mol^{-1}]	Vapor Pressure at 20 °C [hPa]
Benzene	78.11	744.8–750.4 [28–30]	99.5 [31]
Toluene	92.14	782.4–784.0 [28–30]	29.1 [32]
Ethylbenzene	106.17	788.0–789.9 [29,30]	9.5 [33]
p-Xylene	106.17	785.4–794.4 [28–30]	8.7 [34]
1,2,4-Trimethylbenzene	120.19	~837 [35]	2.3 [36]
Naphthalene	128.17	800.0–802.9 [30]	0.08 [37]
n-Hexane	86.18	672.4 [38]	160 [39]
2-Hexanone	100.16	~840 [40]	3.6 [41]
Water	18.02	690 H$^+$(H$_2$O) [42]	23.3 [43]
		808 H$^+$(H$_2$O)$_2$ [42]	

Fig. 2 *Top*: the relationship between the RIP compensation voltage (CV), the RIP area, and the humidity. *Bottom*: the relationship between the RIP compensation voltage, the RIP FWHM, and humidity
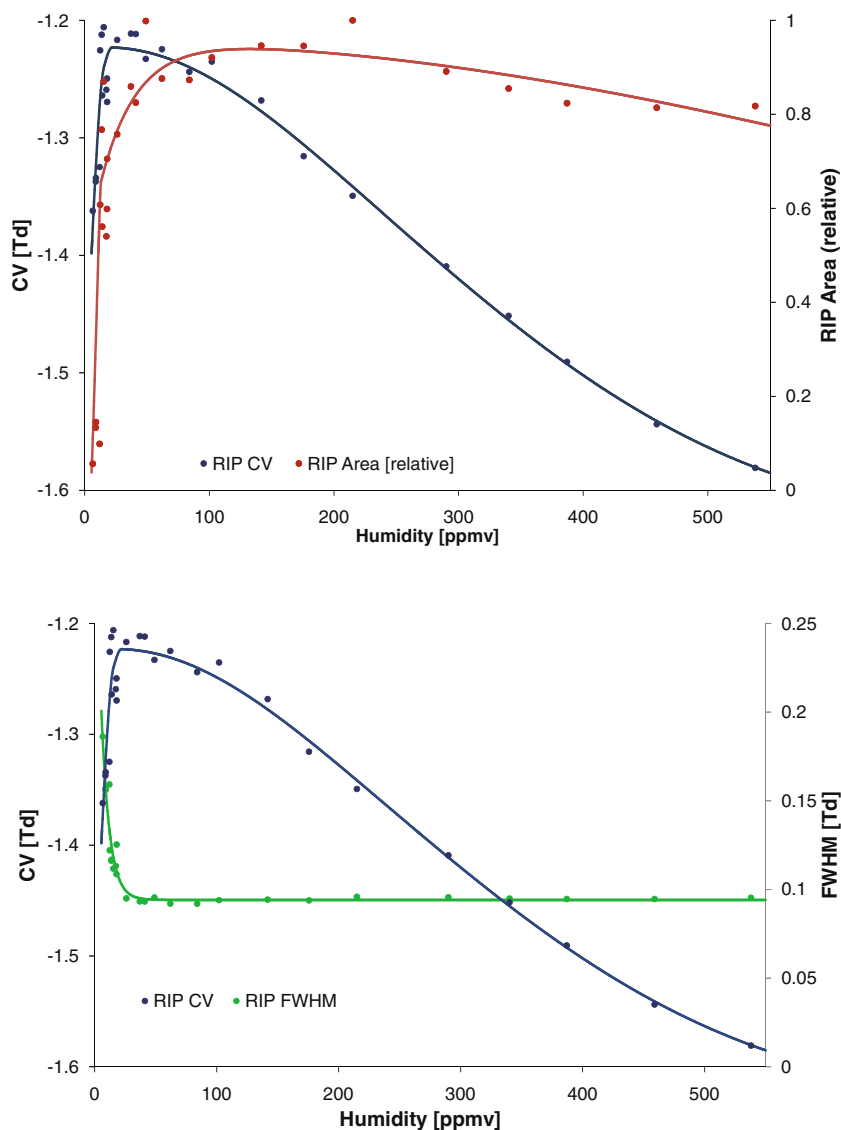

concentration is not high enough for the formation of a significant number of water clusters containing multiple water molecules. Therefore, most of the water clusters are represented by H_3O^+ ($H^+(H_2O)_n$, $n=1$). As a result, no negative RIP compensation voltage shift, typical for the water clusters with higher water content, is observed. The further increase of the water concentration results in an increase of the average water cluster size leading to the shift of the RIP signal toward the negative CV. The shift of the RIP toward the negative CV values can be explained by the reversible cluster formation model, which describes field dependent cluster formations that lead to variation of the average ion cluster cross section [9]. This model demonstrates that water cluster size and the cluster mobility are dependent on the concentration of the clustering particles, cluster temperature, and complex formation energy. With an increase of electric field strength, the effective cluster temperature rises, resulting in a rapid

declustering due to a high collision rate at atmospheric pressure. Hence, the average cluster size is reduced. A reduction in the average cluster size may increase ion mobility significantly. Under a low electric field, a higher water concentration in the gas phase leads to an increase in the average cluster size. An increase in the cluster cross-section, which correlates with the humidity, results in reduced cluster mobility and a corresponding increase in frequency of cluster to carrier gas collisions. As a result, the difference between mobility of the ions in the low and in the high electric fields at a higher humidity increases, leading to increase of the signal shift on the CV scale.

Another feature shown in Fig. 2 (bottom) is the relationship between the RIP FWHM and humidity. Strong reduction of the peak width is observed when humidity is increased to 20 ppm$_v$. This effect takes place in the same humidity range in which the increase of the RIP area and the RIP shift toward

Fig. 3 DMS spectra at humidities of 6.5, 9.0, 12.4, 15.3, 176, 538 ppm$_v$. Insert: the comparison of waveforms at low (*left axis*, 6.5 and 9.0 ppm$_v$) and high (*right axis*, 176 ppm$_v$) humidities
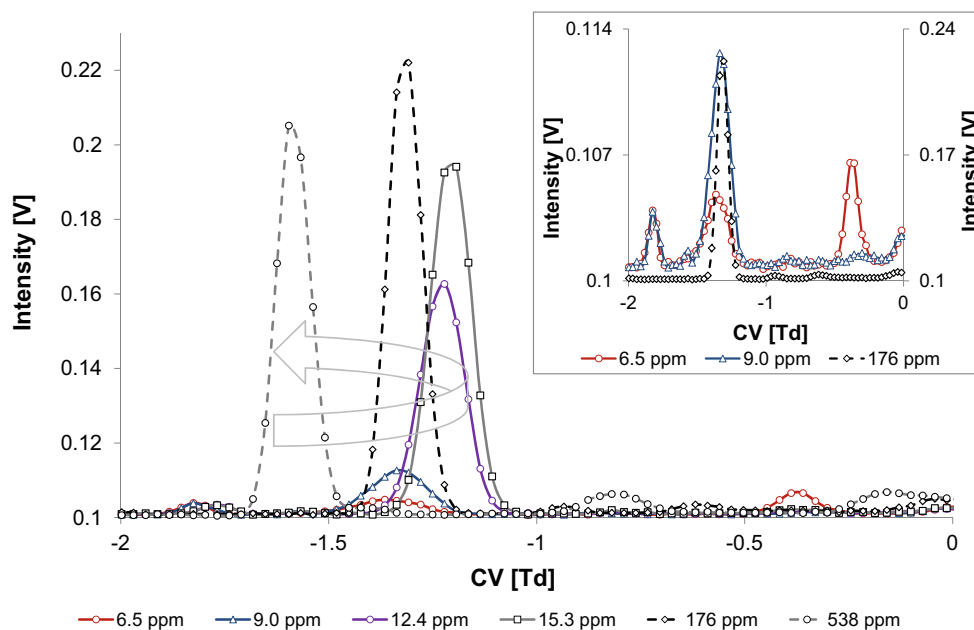
more positive CV values were observed. Therefore, it can be assumed that all these effects have the same nature. The reduction of the RIP width can be explained in context of the proposed model described above. At humidities lower than 20 ppm$_v$ the positive charges are distributed between different charge-carriers, and as a result the peak of the RIP is represented by the superposition of individual charge carrier peaks. This leads to the peak broadening (see waveforms at humidities of 6.5 and 9 ppm, Fig. 3, insert). With the increase in humidity the fraction of the positive charge carriers represented by the protonated water clusters grows. As a result, the peak represented by the protonated water clusters dominates over the peaks of other charge carriers, decreasing the FWHM of the RIP peak. The further increase in humidity (20–550 ppm$_v$) results in the increase of the average cluster size with no change in the ion core nature. In this humidity range, the FWHM of the RIP peak is almost unchanged but the shift of the RIP peak toward more negative CV values is observed. The DMS spectra at humidities of 6.5, 9.0, 12.4, 15.3, 176, 538 ppm$_v$ are presented in the Fig. 3.

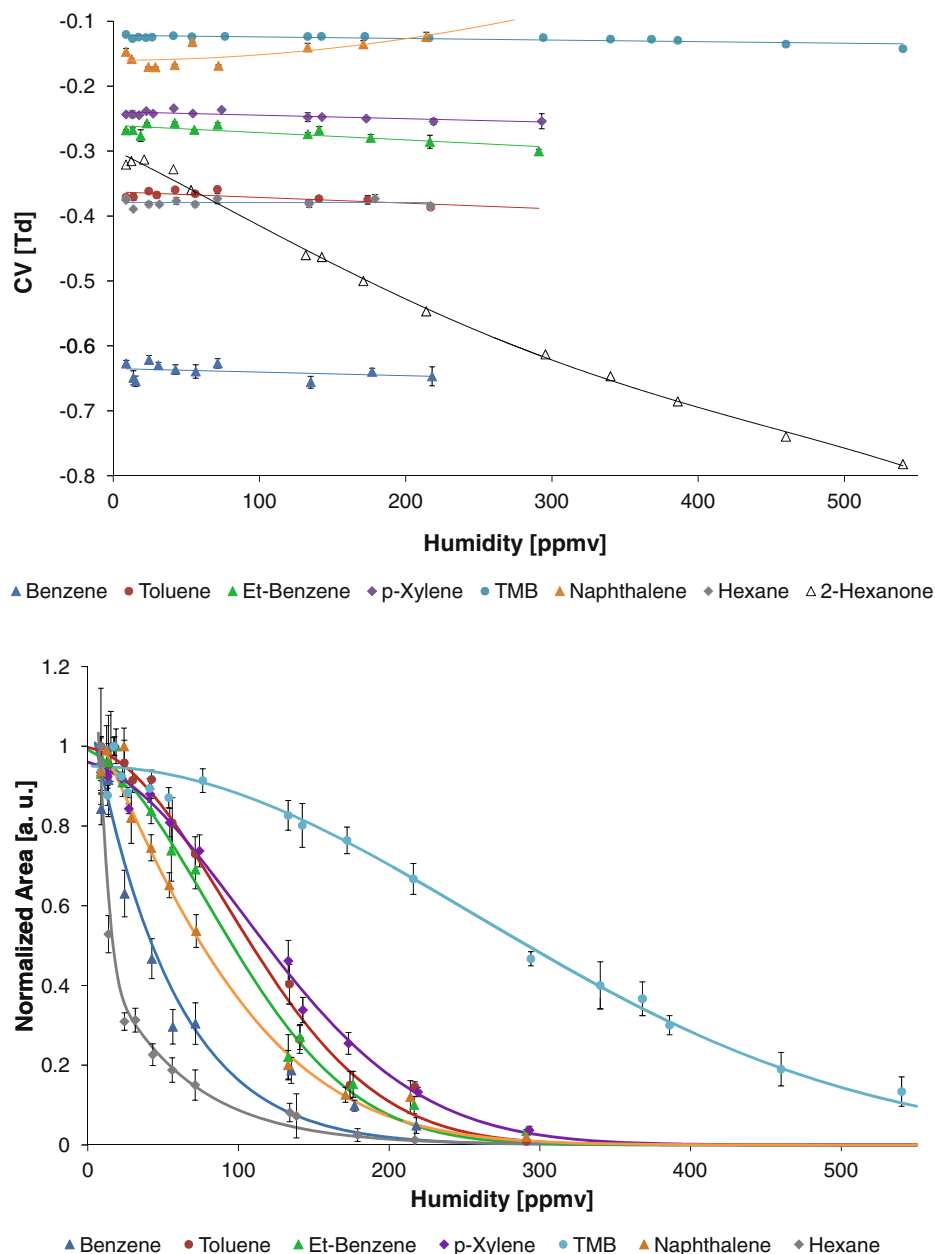Effects of the humidity on the compensation voltage and peak area of model compounds

The effect of humidity on TOF-IMS signal is well investigated [23, 24]. The influence of moisture on the ion-peak compensation voltage, measured with the DMS with the ^{63}Ni-ionization source, was previously investigated on example of organophosphorus compounds by Eiceman et al. [25] and later by Krylov et al. [9]. Significant compensation voltage shift was observed for all tested compounds at humidities higher than 50 ppm.

In contrast to the polar compounds analyzed in previous studies, hexane and all aromatic compounds except of naphthalene demonstrate only a minor change of the peak position on the CV scale with the increase in humidity (see Fig. 4, top). The most likely reason for the humidity independent CV of these compounds is a weak interaction with the water clusters. Due to the weak analyte-ion to water interaction, the analyte-ion size is almost independent of the humidity and no significant dependence of the analyte peak CV on the humidity can be observed.

In the case of naphthalene, the increase in humidity within the range of 8–20 ppm$_v$ results in a slight peak shift toward the more negative CV values. The following increase of the humidity leads to the peak shift toward more positive CV values. Unlike hexane and non-polar aromatic compounds the polar 2-hexanone demonstrates a dependence of the CV on humidity typical for the polar compounds. Due to the strong interaction of 2-hexanone with water clusters, with the increase of humidity, the difference in the ion size during the low and high field portions increases. This results in the peak shift towards more negative CV values.

All of the tested non-polar compounds demonstrate a decrease of the signal area with an increase of the humidity. The effect of the water vapor concentration on the signal intensity of the aromatic compounds is not sufficiently investigated for the DMS-based systems. On the other hand, this effect was described for the proton-transfer-reaction mass spectrometry (PTR-MS). Warneke et al. have observed that the increased concentration of the water leads to a significant reduction of the benzene and toluene signals [26]. Most of the other compounds investigated in this study demonstrate no dependence of the signal on the water vapor concentration. The unusual

Fig. 4 *Top*: the relationship between the compensation voltage (CV) of the model compounds and humidity. *Bottom*: the relationship between the normalized peak area of the model compounds and humidity

▲ Benzene   ● Toluene   ▲ Et-Benzene   ◆ p-Xylene   ● TMB   ▲ Naphthalene   ◆ Hexane   △ 2-Hexanone

▲ Benzene   ● Toluene   ▲ Et-Benzene   ◆ p-Xylene   ● TMB   ▲ Naphthalene   ◆ Hexane

sensitivity of benzene and toluene to moisture was explained by their low proton affinity. At the low water vapor concentration the main proton carrier is $H^+(H_2O)$, which has a proton affinity of 690 kJ mol^{-1}. All of the tested compounds, including benzene and toluene, have a significantly higher proton affinity (see Table 1) and can be efficiently ionized. At higher water vapor concentration the main proton carrier was found to be $H^+(H_2O)_2$, which has a proton affinity of 808 kJ mol^{-1}. Due to the lower proton affinity the ionization of the benzene and toluene is problematic.

The results achieved in this study are in a good agreement with the observation described above. All measured compounds can be divided into three groups according to the proton affinity (see Table 1). Hexane and benzene, which have the lowest proton affinities, demonstrate the strongest decrease of the signal area with increase of humidity. The next group is represented by four compounds: toluene, ethylbenzene, *p*-xylene, and naphthalene. These compounds have proton affinity in the range from 782 to 803 kJ mol^{-1}. The smallest loss of signal area was demonstrated by TMB, which has the highest proton affinity among the analyzed compounds. It is remarkable that TMB signal area decreases by 87 % at water vapor concentration of 540 ppm$_v$. However, in our previous publication we demonstrated that 2-hexanone, which has a proton affinity comparable with the TMB (~840 kJ mol^{-1}), can be analyzed with no significant deviation

of the peak area within the humidity range of 1300–7000 ppm$_v$ [14]. We assume that the reason for this observation is the probable formation of the 2-hexanone/water clusters, which should have a higher proton affinity than that of the non-solvated 2-hexanone. However, to clarify this phenomenon further studies are required.

Effects of the 2-propanol on the compensation voltage and peak area of model compounds

2-Propanol is one of the most frequently used modifiers, which improves the separation ability of DMS for many of the polar organic compounds. The concentration of 2-propanol in the carrier gas used in previous studies is usually ~1.5 % (v/v) [5, 27]. However, even the addition of traces of

2-propanol in the carrier gas results in a disappearance of the peaks of aromatic compounds (see Fig. 5, bottom).

In Fig. 5 the relationships between the compensation voltage, normalized peak area of the model compounds and the concentration of the 2-propanol in the carrier gas are shown. The measurements were conducted with benzene, toluene and ethylbenzene. The analysis of *p*-xylene, naphthalene and TMB was not possible due to the overlapping of the analyt and 2-propanol peaks. The peak of the hexane was not detectable as soon as the 2-propanol was added to the carrier gas.

Within the measured concentration range (0–0.015 %) no significant variations of the compensation voltage of benzene, toluene, and ethylbenzene were observed. These results support the hypothesis discussed above that the utilization of the

Fig. 5 *Top*: the relationship between the compensation voltage (CV) of the model compounds and the concentration of the 2-propanol in the carrier gas. *Bottom*: the relationship between the normalized peak area of the model compounds and the concentration of the 2-propanol in the carrier gas

74

Int. J. Ion Mobil. Spec. (2015) 18:67–75
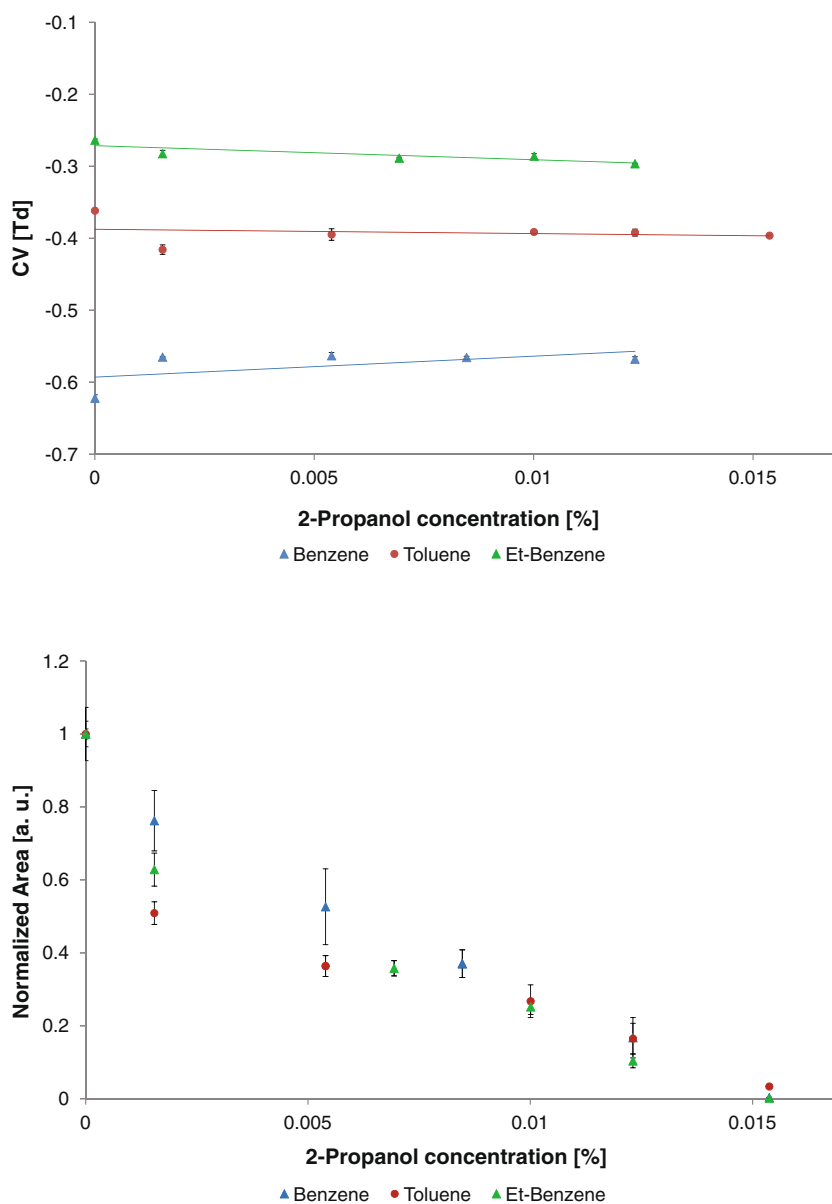
polar modifiers for the non-polar aromatic compounds is not useful or, in some cases, may be even counterproductive.

Conclusion

The influence of the humidity on the analysis of the aromatic compounds with DMS was proven on example of seven model compounds. Six of these compounds represent aromatic compounds (BTEX, TMB, and naphthalene) and one aliphatic compound (hexane). It was demonstrated on example of water vapors and 2-propanol that utilization of the polar modifiers does not improve the separation of aromatic compounds with the DMS. Moreover, the peak area of the model compounds decreases with the increase of the modifier (humidity and 2-propanole) concentration. At water vapor concentration of 300 ppm$_v$ the peaks of all compounds except TMB are no more detectable. The peak of TMB was not detectable at water vapor concentrations higher than 600 ppm$_v$. The remarkable effect, explained by the change of the main charge carrier at the humidity of ~20 ppm, was found during the analysis of the relationships between the RIP peak parameters (area, compensation voltage, FWHM) and the water vapor concentration.

The results presented in this paper demonstrate the importance of the humidity control during the analysis of aromatic compounds with DMS. This is especially important for the analysis of the environmental samples which are usually containing significant humidity level. The increased humidity during the analysis can drastically increase analytes limits of detection resulting in the wrong quantification.

References

1. Baciocchi R, Berardi S, Verginelli I (2010) Human health risk assessment: Models for predicting the effective exposure duration of on-site receptors exposed to contaminated groundwater. J Hazard Mater 181:226–233. doi:10.1016/j.jhazmat.2010.05.001

2. Shih T, Rong Y, Harmon T, Suffet M (2004) Evaluation of the impact of Fuel hydrocarbons and oxygenates on groundwater resources. Environ Sci Technol 38:42–48. doi:10.1021/es0304650

3. Saeed T, Al-Mutairi M (1999) Chemical composition of the water-soluble fraction of the leaded gasolines in seawater. Environ Int 25:117–129. doi:10.1016/S0160-4120(98)00093-2

4. Chary NS, Fernandez-Alba AR (2012) Determination of volatile organic compounds in drinking and environmental waters. Trends Anal Chem 32:60–75. doi:10.1016/j.trac.2011.08.011

5. Schneider BB, Covey TR, Nazarov EG (2013) DMS-MS separations with different transport gas modifiers. Int J Ion Mobil Spectrom 16:207–216. doi:10.1007/s12127-013-0130-8

6. Liang F, Kerpen K, Kuklya A, Telgheder U (2012) Fingerprint identification of volatile organic compounds in gasoline contaminated groundwater using gas chromatography differential ion mobility spectrometry. Int J Ion Mobil Spectrom 15:169–177. doi:10.1007/s12127-012-0101-5

7. Shvartsburg AA (2008) Differential ion mobility spectrometry: nonlinear ion transport and fundamentals of FAIMS. CRC Press, Boca Raton, ISBN-13: 978-1420051063

8. Kolakowski BM, Mester Z (2007) Review of applications of high-field asymmetric waveform ion mobility spectrometry (FAIMS) and differential mobility spectrometry (DMS). Analyst 132:842–864. doi:10.1039/b706039d

9. Krylov EV, Nazarov EG (2009) Electric field dependence of the ion mobility. Int J Mass Spectrom 285:149–156. doi:10.1016/j.ijms.2009.05.009

10. Buryakov IA, Krylov EV, Nazarov EG, Rasulev UK (1993) A new method of separation of multi-atomic ions by mobility at atmospheric pressure using a high-frequency amplitude-asymmetric strong electric field. Int J Mass Spectrom Ion Process 128:143–148. doi:10.1016/0168-1176(93)87062-W

11. Miller RA, Nazarov EG, Eiceman GA, King AT (2001) A MEMS radio-frequency ion mobility spectrometer for chemical vapor detection. Sensors Actuators A Phys 91:301–312. doi:10.1016/S0924-4247(01)00600-8

12. Levin DS, Vouros PA, Miller RA, Nazarov EG, Morris JC (2006) Characterization of gas-phase molecular interactions on differential mobility ion behavior utilizing an electrospray ionization-differential mobility-mass spectrometer system. Anal Chem 78:96–106. doi:10.1021/ac051217k

13. Coy SL, Krylov VE, Nazarov EG, Fornace AJ Jr, Kidd RD (2013) Int J Ion Mobil Spectrom 16:217–227. doi:10.1007/s12127-013-0135-3

14. Kuklya A, Uteschil F, Kerpen K, Marks R, Telgheder U (2014) Development of an electrospray-^{63}Ni-differential ion mobility spectrometer for the analysis of aqueous samples. Talanta 120:173–180. doi:10.1016/j.talanta.2013.10.056

15. Eiceman GA, Krylov EV, Krylova NS, Nazarov EG, Miller RA (2004) Separation of ions from explosives in differential mobility spectrometry by vapor-modified drift gas. Anal Chem 76:4937–4944. doi:10.1021/ac035502k

16. Rorrer LC III, Yost RA (2011) Solvent vapor effects on planar high-field asymmetric waveform ion mobility spectrometry. Int J Mass Spectrom 300:173–181. doi:10.1016/j.ijms.2010.04.002

17. Schneider BB, Covey TR, Coy SL, Krylov EV, Nazarov EG (2010) Control of chemical effects in the separation process of a differential mobility mass spectrometer system. Eur J Mass Spectrom 16:57–71. doi:10.1255/ejms.1025

18. Purves RW, Guevremont R, Day S, Pipich CW, Matyjaszczyk MS (1998) Mass spectrometric characterization of a high-field asymmetric waveform ion mobility spectrometer. Rev Sci Instrum 69:4094–4105. doi:10.1063/1.1149255

19. Kolakowski BM, McCooeye MA, Mester Z (2006) Compensation voltage shifting in high-field asymmetric waveform ion mobility spectrometry-mass spectrometry. Rapid Commun Mass Spectrom 20:3319–3329. doi:10.1002/rcm.2739

20. Wojdyr M (2010) Fityk: a general-purpose peak fitting program. J Appl Crystallogr 43:1126–1128. doi:10.1107/S0021889810030499

21. Nazarov EG, Coy SL, Krylov EV, Miller RA, Eiceman GA (2006) Pressure effects in differential mobility spectrometry. Anal Chem 78:7697–7706. doi:10.1021/ac061092z

22. Kim SH, Betty KR, Karasek FW (1978) Mobility behavior and composition of hydrated positive reactant ions in plasma chromatography with nitrogen carrier gas. Anal Chem 50:2006–2012. doi:10.1021/ac50036a018

23. Mäkinen M, Sillanpää M, Viitanen A-K, Knap A, Mäkelä J, Puton J (2011) The effect of humidity on sensitivity of amine detection in ion

mobility spectrometry. Talanta 84:116–121. doi:10.1016/j.talanta.2010.12.030

24. Mayer T, Borsdorf H (2014) Anal Chem 86:5069–5076. doi:10.1021/ac5007393

25. Krylova N, Krylov E, Eiceman GA, Stone JA (2003) Effect of moisture on the field dependence of mobility for gas-phase ions of organophosphorus compounds at atmospheric pressure with field asymmetric ion mobility spectrometry. J Phys Chem A 107:3648–3654. doi:10.1021/jp0221136

26. Warneke C, van der Veen C, Luxembourg S, de Gouw JA, Kok A (2001) Measurements of benzene and toluene in ambient air using proton-transfer-reaction mass spectrometry: calibration, humidity dependence, and field intercomparison. Int J Mass Spectrom 207:167–182. doi:10.1016/S1387-3806(01)00366-9

27. Schneider BB, Nazarov EG, Covey TR (2012) Peak capacity in differential mobility spectrometry: effects of transport gas and gas modifiers. Int J Ion Mobil Spectrom 15:141–150. doi:10.1007/s12127-012-0098-9

28. Chong S-L, Franklin JL (1972) Proton affinities of benzene, toulene, and the xylenes. J Am Chem Soc 94:6630–6635. doi:10.1021/ja00774a010

29. Hunter EPL, Lias SG (1998) Evaluated gas phase basicities and proton affinities of molecules: an update. J Phys Chem Ref Data 27:413–656. doi:10.1063/1.556018

30. Auea DH, Guidonia M, Betowski LD (2000) Ab initio calculated gas-phase basicities of polynuclear aromatic hydrocarbons. Int J Mass Spectrom 201:283–295. doi:10.1016/S1387-3806(00)00210-4

31. Benzene (2013) MSDS, version 5.1; Sigma-Aldrich, Oct 17

32. Toluene (2014) MSDS, version 5.4; Sigma-Aldrich, Jan 29

33. Ethylbenzene (2010) MSDS, version 10.1; Merck, Nov 04

34. p-Xylene (2014) MSDS, version 9.3; Merck, May 15

35. Zhao J, Zhang R (2004) Proton transfer reaction rate constants between hydronium ion (H_3O^+) and volatile organic compounds. Atmos Environ 38:2177–2185. doi:10.1016/j.atmosenv.2004.01.019

36. 1,2,4-Trimethylbenzene, MSDS, version 5.1; Sigma-Aldrich, Jul 04, 2013

37. Naphthalene (2010) MSDS, RN 1; Acros, Sep 27

38. Hunter KC, East ALL (2002) Properties of C−C Bonds in n-Alkanes: relevance to cracking mechanisms. J Phys Chem A 106:1346–1356. doi:10.1021/jp0129030

39. n-Hexane (2014) MSDS, version 18.0; Merck, Apr 14

40. Blake RS, Patel M, Monks PS, Ellis AM, Inomata S, Tanimoto H (2008) Aldehyde and ketone discrimination and quantification using two-stage proton transfer reaction mass spectrometry. Int J Mass Spectrom 278:15–19. doi:10.1016/j.ijms.2008.07.010

41. 2-Hexanone (2006) MSDS, version 1.0; TCI, Apr 04

42. Goebbert DJ, Wentold PG (2004) Water dimer proton affinity from the kinetic method: dissociation energy of the water dimer. Eur J Mass Spectrom 10:837–846. doi:10.1255/ejms.684

43. Water (2012) MSDS, RN 4; Acros, Jun 15